Study on convective heat transfer coefficient around a circular jet ejected into a supersonic flow

J.J. Yi[1], J.W. Song[1], M.S. Yu[2], and H.H. Cho[3]

[1] *Graduate school of Mechanical Engineering, Yonsei University 120-749, Republic of Korea*
[2] *Graduate school of Mechanical Engineering, Yonsei University, presently National Science Museum Planning Office, Ministry of Science and Technology, 427-060, Republic of Korea*
[3] *Mechanical Engineering, Yonsei University 120-749, Republic of Korea*

1 Introduction

The secondary jet injection into a supersonic cross flow can be observed in various situations such as a thrust vector control of a rocket and fuel injection of a scramjet engine, etc. The secondary jet in a supersonic flow acts as blocking body to the approaching cross flow although it is a fluid. When the blocking body exists in a supersonic flow, a complex structure of shock waves is produced. Many investigations have been conducted about the blocking bodies in a supersonic flow. Schuricht and Roberts[3] took surface temperature images using a TLC (Thermochromic Liquid Crystal) thermography to calculate the convective heat transfer coefficient. Yu[4] has measured the heat transfer coefficient around a protuberant cylinder body in supersonic flow by using a infra-red camera. There are some papers published about the pressure distribution around secondary injection hole in supersonic flow. Everett[5] has measured the pressure distribution around the circular secondary injection hole using PSP (Pressure Sensitive Paint), which show that the maximum pressure appeared on the side of injection hole. Huang[6] reported the crescent shape dimple around secondary injection hole which is installed at Titan IV SRM nozzle. Huang concluded that the high pressure and heat transfer cause the ablation around secondary injection. Although there are lots of studies on flow field and heat transfer about the cylindrical body and fin, there is little information about the heat transfer around a secondary jet. In this study, the convective heat transfer coefficient was measured around a circular secondary jet ejected into the supersonic flow field. The wall temperature measurement around the injection nozzle was conducted using an infra-red camera. A constant heat flux was applied to the wall around the secondary nozzle. For the different jet to freestream momentum ratio, the stagnation pressure of the secondary injection was controlled. The measured temperature is used to calculate the convective heat transfer coefficient. The comparison of the heat transfer coefficient distribution and the pressure distribution which is measured by Everett[5] was made in the center line.

2 Experimental facilities and data reduction

2.1 Supersonic blow-down tunnel

A supersonic blow-down tunnel was made for this test. In experimental facilities, there is the high pressure flow supplement system consisting of air compressor, coolers, filters, and air tanks. The air is compressed up to about 200atm. The compressed air is stored about 150atm in air storage tanks which has a $1.8m^3$ storage capacity. In the test, the compressed air is supplied from storage tanks to the stagnation chamber lowering the

pressure level down to 6.8atm by a pressure regulator. In the inlet diffuser of stagnation chamber, there are a cone-type separator and 5-stage screen installed for lowering the turbulence level and increasing the flow uniformity. The pressure and temperature in stagnation chamber are measured during the experiments. Figure 1 shows the pressure and temperature in freestream stagnation chamber. Stabilized air is passed through the nozzle for accelerating velocity to Mach 3. The accelerated air enters the test chamber. The test model which is placed in test chamber goes through the supersonic field. In test chamber, the static pressure was measured at 0.17atm. From the secondary injection tank, the air is passed through the pressure regulator lowering the adequate pressure for fitting the jet to freestream momentum ratio. In the secondary injection stagnation chamber, the air is stabilized and the stagnation pressure is measured. In the test model, there is the secondary flow passage for guiding the flow to test surface.

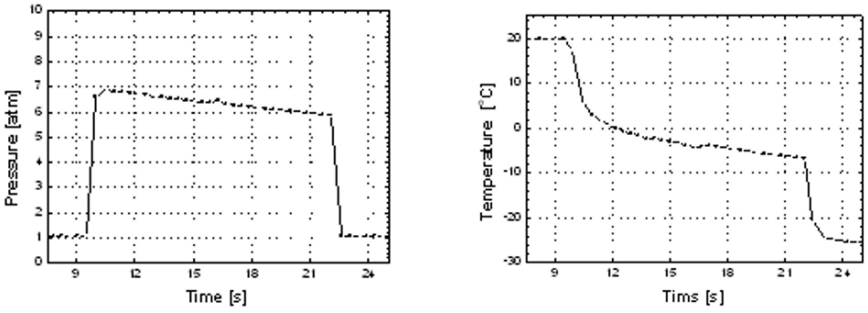

Fig. 1. The stagnation pressure and temperature at freestream stagnation chamber

2.2 Test model and other supplement equipments

Figure 2 shows the test model and the electrical foil heater in the experiment of the secondary injection. The considered surface where the secondary injection hole is located and the temperature was measured was placed on the electrical foil heater to satisfy the constant heat flux condition. At the back of the heater, a 5mm thickness Teflon block was placed to prevent the heat loss. For uniform constant heat flux condition around the secondary injection. The foil heaters resistance which was employed in the secondary injection experiment is 267Ω. The electrical source of the heater is the direct current supplied by the electrical power (200V, 20A). The supplied current value was monitored during the test by checking the voltage drop across the shunt placed in the middle of the electrical circuit. Most of voltage signals from sensors such as pressure transducers and thermocouples are received by the voltmeter (Agilent, HP34970A) and processed in a computer. The surface temperature on a considered surface was measured using the infra-red camera (Jenoptik, Varioscan3011-ST). The error estimation is 13.39 %. The major errors were caused by heat loss to the back of test and the heat resistance. The surface temperature was measured by the infra-red camera which was installed at the upper wall of test chamber. The secondary flow enters through the passage installed below of the test model surface. The secondary flow reached the Mach number 1 when it passed through the secondary flow nozzle, satisfying the chocking condition.

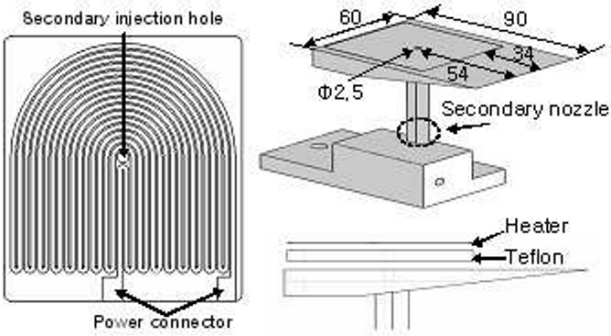

Fig. 2. The test model and heater pattern

2.3 Experimental condition and data reduction

The experiments were conducted under the constant heat flux condition on a considered surface. The freestream Mach number was about 3 and the unit Reynolds number was about $5.0 \times 10^7/m$. During the experiments, the stagnation chamber pressure was almost maintained to be 6.3atm although the chamber temperature decreased gradually due to the gas expansion in storage tanks and the Joule-Thomson effect at the valves and the pressure regulator. The heat flux was fixed at about 30,000 W/m^2. The heat flux value was calculated applying the following Eq. 1

$$\dot{q} = \dot{q}_h - \dot{q}_l \tag{1}$$

$\dot{g}_h$ is the heat generation of heater and it can be calculated using Eq. 2

$$\dot{q}_h = I^2 R \tag{2}$$

I is the current which is supplied heater and R is the heater resistance. $\dot{q}_l$ is the heat loss in the backward of test surface. The heat loss was estimated by the analysis of the one dimensional transient conduction problem and the flat surface condition was applied as boundary condition. The heat loss analysis process was conducted by the commercial code, Fluent vs. 6.2.16. When about 30,000W/m^2 heat is generated by the heater, the total heat loss was calculated to 6 % of the total heat flux. The heat transfer coefficient is calculated using Eq. 3

$$h = \frac{\dot{q}}{T_w - T_{aw}} \left[1 - \left(\frac{\xi}{x} \right)^{0.9} \right]^{-\frac{1}{9}} \tag{3}$$

where, T_{aw} was calculated by Eq. 4

$$T_{aw} = T_0 \frac{1 + r\frac{k-1}{2} Ma_\infty^2}{1 + \frac{k-1}{2} Ma_\infty^2} \tag{4}$$

The recovery factor, , is $Pr_{air}^{1/3}$. For controlling the jet to freestream momentum ratio, the secondary stagnation pressure was controlled by the pressure regulator. Equation 5 shows the definition of jet to freestream momentum ratio.

$$J = \frac{(\rho V^2)_j}{(\rho V^2)_\infty} = \frac{(\gamma p M a)_j}{(\gamma p M a)_\infty} \tag{5}$$

In the experiment, the freestream Mach number and the static pressure at the test chamber were 3 and 0.17atm, respectively. The static pressure at the secondary injection hole was governed by the stagnation pressure at the secondary injection stagnation chamber.

3 Results

3.1 The oil streak pattern

The experiments about the oil streak pattern were conducted with respect to jet to freestream momentum ratio. Figure 3 shows the results of the oil streak pattern. When the jet to freestream momentum ratio was increased, the length of the first separation and second separation was increased. When the jet to freestream momentum ratio was 1.17, the first separation length in a center line was expected to occur at about 2.25D upstream of secondary injection hole diameter and the second separation distance in center line was 1.2D upstream of secondary injection hole diameter. When the jet to freestream momentum ratio was 2.15, the first separation line appeared on 3.5D and the second separation line was believed to occur at about 1.6D upstream of the secondary injection hole diameter. When the jet to freestream momentum ratio was increased, the separation length was far from the secondary injection hole. The reason of this flow separation is known to be the reverse gradient of a surface pressure in a flow direction. When the momentum ratio increases, the surface pressure behind the inviscid shock wave around the secondary injection hole is increased and it could be propagated further upstream. This upstream pressure propagation is thought to cause the earlier flow separation for the higher jet to freestream momentum ratio.[7]

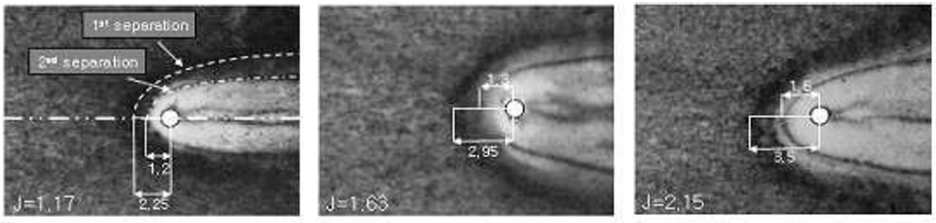

Fig. 3. The results of the oil streak pattern with respect to jet to freestream momentum ratio

3.2 Heat transfer coefficient

Figure 4 shows the contours of the convective heat transfer coefficient with respect to the jet to freestream momentum ratio on the surface of the test model. In Fig. 4, the

white circle in the middle of all figures represents the secondary injection hole. From the leading edge of the test model to the first separation, the convective heat transfer coefficients have the tendency to decrease because of the development of the boundary layer. Behind the first separation line, the heat transfer coefficient increases. Also, when the jet to freestream momentum ratio increases, the heat transfer coefficient around the secondary injection hole increases. As shown in the figure, the maximized region of the heat transfer coefficient appears on the both sides of the secondary injection hole. Figure 5 shows the comparison between heat transfer and surface pressure. In the case of the surface pressure distribution, the results of Everett[5] were referred. Everett conducted the pressure measurement test using PSP (Pressure Sensitivity Paint) for various jet to freestream momentum ratios such as 1.2, and 2.2. In this study, the jet to freestream momentum ratios were 1.17, and 2.15. Therefore, two results can be compared each other qualitatively. In Fig.5.a, the jet to freestream momentum ratios of the heat transfer coefficient and pressure distribution are 1.17 and 1.2, respectively. Two distributions of heat transfer coefficient and surface pressure show a similar pattern each other although the heat transfer coefficient doesn't show any change in the pressure plateau region. The maximum values of heat transfer coefficient and surface pressure appear similarly just in front of an injection hole. The same results appear in Fig. 5.b. In the Fig.5.b the jet to freestream momentum ratios of the heat transfer coefficient and pressure distribution are 2.15 and 2.2, respectively. The value of the convective heat transfer coefficient and

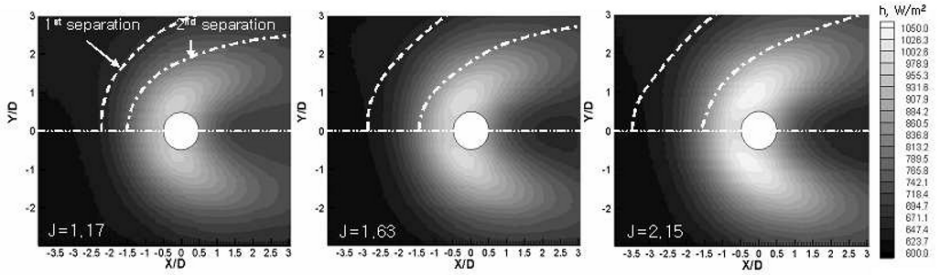

Fig. 4. The results of the convective heat transfer coefficient with respect to jet to freestream momentum ratio

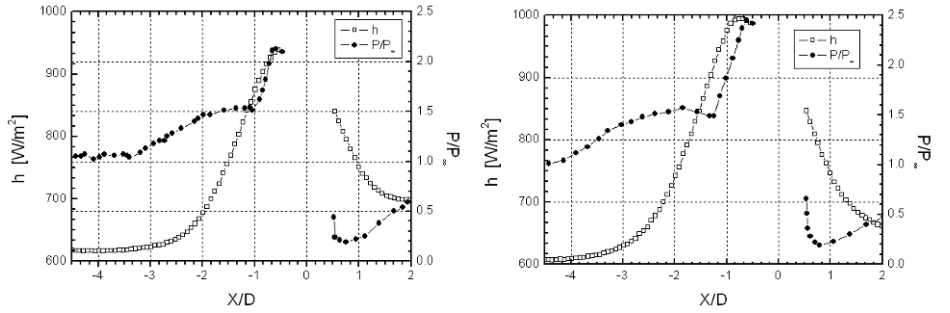

Fig. 5. The comparison between the heat transfer coefficient and pressure distribution in a center line, $a.J = 1.17(left), b.J = 2.15(right)$

the pressure was increased with respect to jet to freestream momentum ratio. The peak point locations of the heat transfer coefficient and the surface pressure are observed at the almost same position.

4 Conclusion

The measurement of the convective heat transfer coefficient was conducted for the flat surface where the secondary jet was ejected into the supersonic cross-flow. Also, the comparison between the heat transfer coefficient distribution and surface pressure distribution along the center line was performed. The results of the oil streak pattern around the circular secondary injection hole showed that the separation length was increased with increasing the jet to freestream momentum ratio. In this turbulent flow separation region, the surface heat transfer is promoted and the effected region becomes larger with increasing jet to freestream momentum ratio. Surface pressure shows a similar pattern with the surface heat transfer coefficient and has the peak value at the same position where the maximum heat transfer coefficient appears.

References

1. Hung, F. T., and Clauss, J. M. : Three-Dimensional Protuberance Interference Heating in High-Speed Flow. AIAA Paper 80-0289, Jan. 1980
2. Aso, S., Hayashi, M., and TAN, A. : Aerodynamic heating phenomena in three dimensional shock wave/turbulent boundary layer interactions induced by sweptback blunt fins. AIAA 28th Aerospace Sciences Meeting, AIAA-1990-381, AIAA, Washington D.C.
3. Schuricht, P.H., and Roberts, G. T. : Hypersonic interference heating induced by a blunt fin. AIAA 8th International Space Planes and Hypersonic System and Technologies Conference, AIAA-1998-1579, AIAA, Washington D.C.
4. Yu, M.S., Yi, J.J., Cho, H.H., Hwang, G.Y. and Bea, J.C. : A Study of the heat transfer around a cylindrical body protruded into a supersonic flow-field. AJCPP2006-22143, 2006
5. Everett, D.E., Morris, M.J., Wall pressure measurements for a sonic jet injected transversely into a supersonic crossflow : Journal of Propulsion and Power, Vol. 14, No. 6, November-December, pp. 861-868, 1998
6. Huang. W.M., Mistrek, D.L., and Murdock J.W. : Nozzle erosion induced by thrust vector control injection, AIAA paper 96-2638, 1996
7. Stollery, J.L. : Glancing shock-boundary layer interactions, AGARD-R-764, 1990